Fibers and Polymers 2014, Vol.15, No.1, 101-107 DOI 10.1007/s12221-014-0101-7

Preparation of Poly(vinyl alcohol)/Silver-Zeolite Composite Hydrogels by UV-Irradiation

Min Jae Kim, Tae Hwan Oh[1]*, Sung Soo Han[1], Sang Woo Joo[2], Han Yong Jeon[3], and Dong Wook Chang[4]

Korea Textile Development Institute, Daegu 703-712, Korea
[1]*Department of Nano, Medical & Polymer Materials, Yeungnam University, Gyeongsan 712-749, Korea*
[2]*School of Mechanical Engineering, Yeungnam University, Gyeongsan 712-749, Korea*
[3]*Division of Nano-Systems Engineering, Inha University, Incheon 402-751, Korea*
[4]*Department of Chemical Systematic Engineering, Catholic University of Daegu, Gyeongsan 712-702, Korea*
(Received March 26, 2013; Revised May 21, 2013; Accepted May 23, 2013)

Abstract: Poly(vinyl alcohol) (PVA)/Ag-zeolite nanocomposite hydrogels were prepared by UV irradiation using PVA solution mixed with Ag-zeolite nanoparticles. Physical properties and changes in morphology of the PVA/Ag-zeolite hydrogels were investigated. The PVA/Ag-zeolite hydrogels were prepared at a PVA concentration of 9 wt% with a UV irradiation distance of 15 cm, where gel fraction and swelling ratio were optimized. Hardness of the PVA/Ag-zeolite hydrogels decreased with increasing amounts of Ag-zeolite, reaching that of soft elastomer when the amount of Ag-zeolite was 5 % by weight. The PVA/Ag-zeolite hydrogels showed strong antimicrobial activities against *Staphylococcus aureus* and *Klebsiella pneumoniae*, inducing a reduction of bacteria of over 99.9 % at a Ag-zeolite content of 3 wt%.

Keywords: PVA, Ag-zeolite, Hydrogels, UV irradiation, Antimicrobial activities

Introduction

Poly(vinyl alcohol) (PVA) is a representative water soluble polymer that forms both chemical and physical gels when added to aqueous solution depending on preparation conditions [1-5]. PVA hydrogels have been used in biomedical applications such as implants, embolic materials, soft contact lenses, and artificial organs [6,7] because of their inherent non-toxicity, good biocompatibility, non-carcinogenicity, and desirable physical properties. Their rubbery or elastic nature and high swelling ratio in aqueous solutions are good for biomedical applications [8]; therefore, PVA hydrogels have also gained wide pharmaceutical acceptance as drug-delivery matrices or been used in the form of powder added mixtures for manufacturing tablets. PVA hydrogel also has excellent transparency, biologically inactivity and biocompatibility. Thus, it has been widely used for temporary skin covers or burn dressings [9].

Chemical gels are formed using cross-linking agents and radiation of γ or electron rays, whereas physical gels are formed by crystallization, ion bonding and hydrogen bonding [10,11]. Hydrogels have generally been prepared by chemical crosslinking; however, crosslinking agents used for hydrogel preparation may have side effects for biomedical applications and residual substances may remain in the hydrogels.

PVA hydrogels produced by ultraviolet (UV) irradiation techniques can form a matrix having crosslinked polymeric chains without some defects of chemically crosslinked hydrogel using chemical crosslinking agents. Crosslinking by UV irradiation is simple and cost effective when compared to other methods that use γ or electron rays [12-17].

Heavy-metal ions substituted zeolite composed of aluminosilicates is good candidate as effective antibacterial agent, which has a tetrahedron structure of SiO_4 and AlO_4. The heavy-metal ions such as silver (Ag) substituted zeolite has antibacterial activity [18-22] and is also known to be non-toxic to human [23-25].

In this study, chemical crosslinking agent free PVA/Ag-zeolite nanocomposites hydrogels were prepared by UV irradiation, and their physical properties and morphological changes were investigated to identify the optimum manufacturing conditions.

Experimental

Materials and Sample Preparation

PVA with a number-average degree of polymerization (P_n) and degree of saponification (DS) of 1,700 and 99.9 %, respectively, was purchased from DC Chemical Co., Ltd. (Korea). Nano colloidal Ag-zeolite (AGZS-WP0130CA) composed of zeolite of 300,000 ppm and Ag of 10,000 ppm, was purchased from Miji Tech Co., Ltd. (Korea). The particle sizes of Ag and zeolite nanoparticles in the colloidal solution were 5-10 nm and 50±10 nm, respectively. Distilled water was used as a solvent.

Initially, homo PVA were dissolved in water at 90 °C for 2 h and then maintained for 30 min to enhance homogenization. Aqueous solution with PVA polymer concentrations of 5, 7, and 9 wt% were prepared. The solutions were poured into Petri dishes at room temperature and then kept at room temperature for 24 h to remove air bubbles, after which PVA

*Corresponding author: taehwanoh@ynu.ac.kr

hydrogels were prepared by UV-irradiation. To accomplish this, the PVA solutions were exposed to UV irradiation for 10, 20, and 30 min, respectively. The distance of UV irradiation was set at 15 cm, which was determined to be best for gel formation based on repeated tests. Light source was a high pressure mercury ultra-violet lamp with intensity of 180 mW/cm^2 at irradiation distance of 10 cm. A principal wavelength of the UV lame was 365 nm, which is generally used for photo crosslinking of polymer chains [26]. After UV irradiation, the solutions were frozen at −20 °C for 1h, and then at −40 °C for 24 h. The samples were then exposed to hot distilled water at 40 °C for 48 h, followed by vacuum drying at 60 °C for 48 h until they reached constant weight.

To make PVA/Ag-zeolite nanocomposite hydrogels, the concentration of PVA was fixed at 9 wt%. The PVA solutions were prepared in distilled water at 90 °C for 3 h, after which they were cooled to room temperature. Ag-zeolite nanoparticles were dispersed in distilled water under magnetic stirring for 4 h, and the solutions were then sonicated for 4 h at room temperature to enhance dispersion of the particles. The PVA and Ag-zeolite nanocomposite solutions were mixed at 90 °C for 3 h with gentle stirring, and then cooled to room temperature. The Ag-zeolite contents varied by 1, 3, and 5 % by weight based on PVA. PVA/Ag-zeolite hydrogels by UV irradiation were prepared with the same procedure of homo PVA hydrogel as above mentioned. The shape of hydrogel was round plate, of which the thickness and the diameter were 3 mm and 4 cm, respectively.

The gel fraction (cross-linking) was calculated by following equation:

$$\textit{Gel fraction (\%)} = \frac{W_d}{W_i} \times 100 \quad (1)$$

where, W_d is the dried gel weight after extraction, and W_i is the initial weight of the samples.

After vacuum drying at 60 °C, the dried hydrogels were soaked in distilled water at 40 °C for 48 h, then swelling continued until constant weight was reached. the swollen hydrogels (W_s), water on the gel surface was removed with filter paper. Finally, the swelling ratio was calculated using the following formula.

$$\textit{Swelling ratio (\%)} = \frac{W_s - W_d}{W_d} \times 100 \quad (2)$$

where, W_s is the swollen hydrogels weight.

Characterization

Field emission scanning electron microscopy (FE-SEM, S-4100, Hitachi Co., Ltd., Japan) after gold coating was used to investigate morphologies. The compositional elements of PVA/Ag-zeolite nanocomposite hydrogel were analyzed by energy-dispersive X-ray spectrometry (EDS, EMAX, Horiba Co., Ltd., Japan). Transmission electron microscopy (TEM) images were obtained with H-7600 (Hitachi Co. Ltd., Japan) using samples deposited on carbon coated copper grids. Fourier transform infrared (FT-IR) spectra were scanned between 600 and 4000 cm^{-1} with FT-IR (IS-10, Thermo, USA). Thermal behavior was investigated by differential scanning calorimetry (DSC, TA Instrument 2010, USA). The DSC thermograms were recorded from 0 to 260 °C at a heating rate of 10 °C/min under a nitrogen atmosphere.

Antimicrobial activities of the hydrogel were examined against *Staphylococcus aureus* (ATCC 6538P; a Gram-positive bacterium) and *Klebsiella pneumoniae* (ATCC 4352; a Gram-negative bacterium). The bacteria were cultured at 37 °C for the blank control (PVA) and test specimen (PVA/Ag-zeolite), respectively. After culturing the bacteria for 18 h, the number of the bacteria was counted. The reduction of bacteria in the specimen was calculated according to the following equation:

$$\textit{Reduction of bacteria (\%)} = \frac{M_a - M_b}{M_a} \times 100 \quad (3)$$

where, M_a and M_b are the numbers of viable bacteria after cultivation on agar plates for 18 h for the blank control (PVA) and test specimen (PVA/Ag-zeolite), respectively. A Shore D durometer (TH210, Time Group Inc., China) of was used to measure the hardness of the hydrogel and determine the Shore D hardness value.

Results and Discussion

Figure 1 shows the schematic of PVA hydrogel preparation and reactions by UV irradiation. Polymer radical formation mechanisms by irradiation were suggested by many authors [12-17]. The radicals in PVA chain can be formed both directly and indirectly by abstracting hydrogen atoms of PVA chains. The H and OH radicals resulted from irradiation of water molecules can abstract the hydrogen atoms of secondary and tertiary carbons of PVA chains [12-15]. OH radicals can also be formed by reacting degraded polymer chain radical with oxygen [12-15].

The gel fraction and swell ratio of homo PVA hydrogels prepared by UV-irradiation with different PVA concentrations (5, 7, and 9 wt%) are shown in Figure 2. The gel fraction of the PVA hydrogel increased slightly with irradiation time, and it depended more on the PVA concentrations. Higher polymer concentrations induced increased crosslinking points due to higher entanglements of molecular chains. UV-irradiation induced a three-dimensional network structure capable of holding water. The swell ratio increased with increasing PVA concentration, but showed a maximum after irradiation for 10 min, after which it decreased after UV-irradiation for 30 min. These findings indicate that increased cross-linking density induces higher swelling capacity to some extent. However, after reaching the maximum swelling capacity, the excessive UV-irradiation led to a decreased swell ratio due to disrupted network structure as shown in

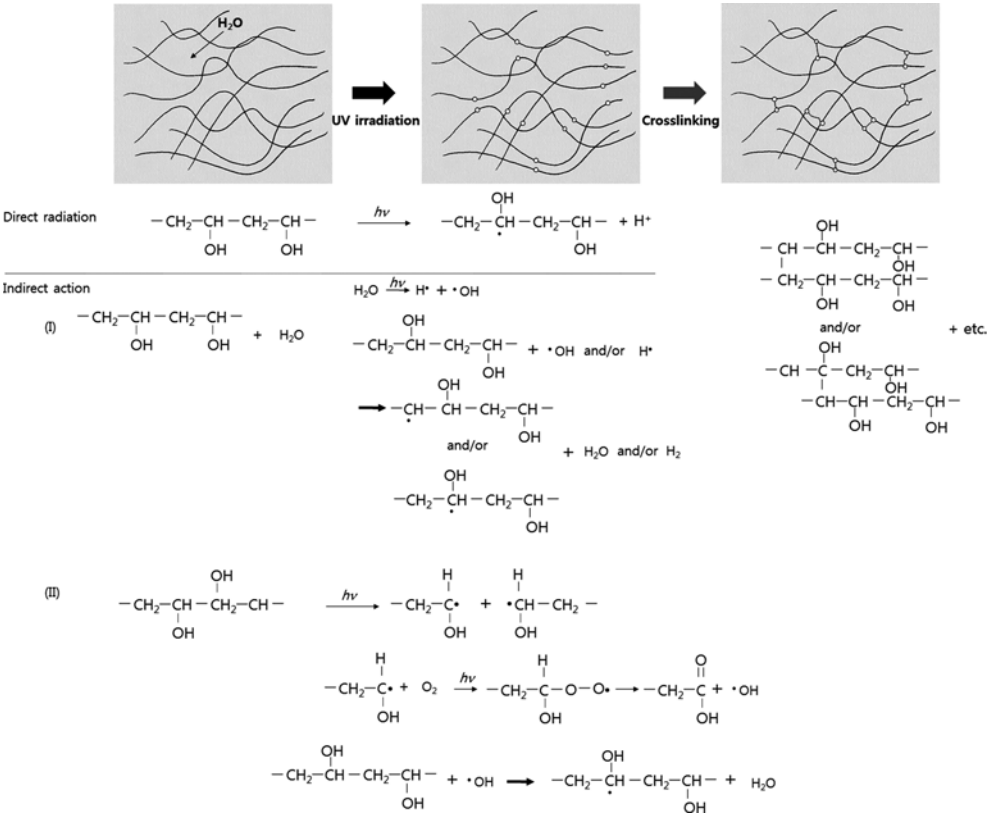

Figure 1. Schematic of PVA hydrogel formation and chemical reactions by UV irradiation.

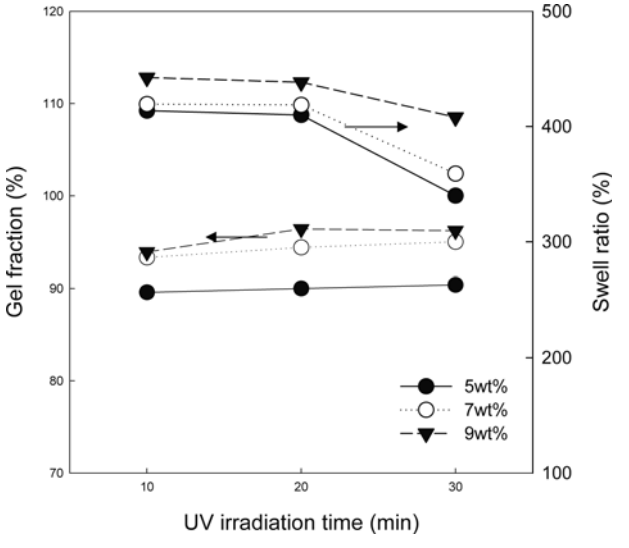

Figure 2. Gel fraction and swell ratio of PVA hydrogel as a function of UV irradiation time.

Figure 3. Accordingly, hydrogels with the same gel fraction can show different swelling behavior depending on the crosslinking density, which varies with UV-irradiation time and polymer concentration.

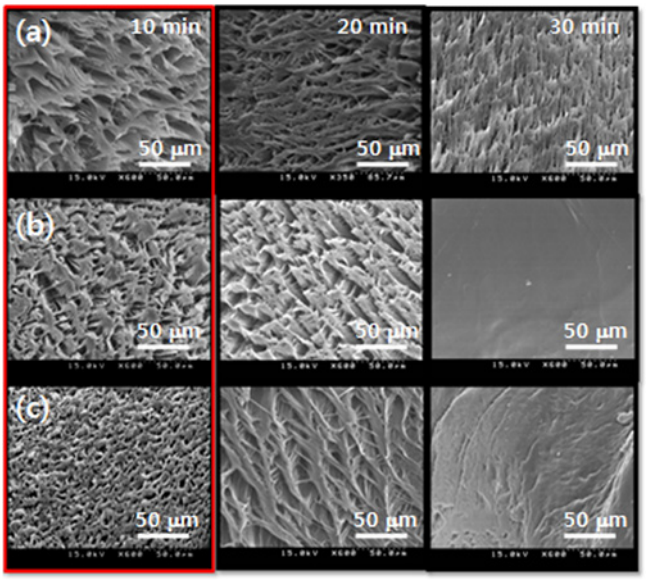

Figure 3. SEM photographs of UV irradiated PVA hydrogels; PVA concentration of (a) 5 wt%, (b) 7 wt%, and (c) 9 wt%.

Figure 3 shows SEM images of PVA hydrogel for different polymer concentrations and irradiation time, and reveals

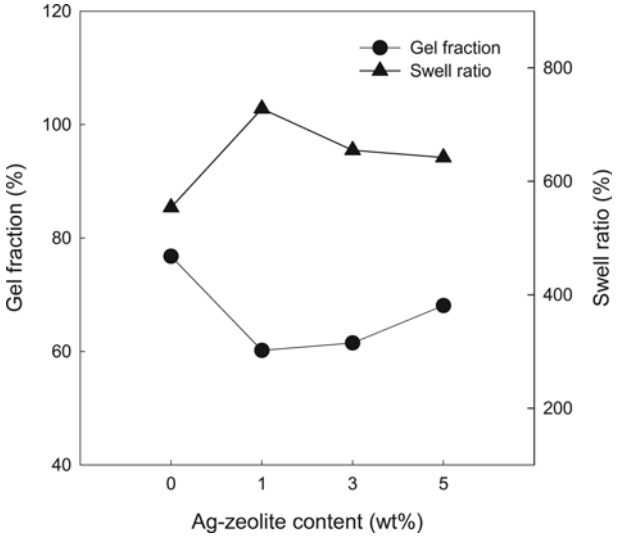

Figure 4. Gel fraction and swell ration of PVA/zeolite composite hydrogel as a function of Ag-zeolite content.

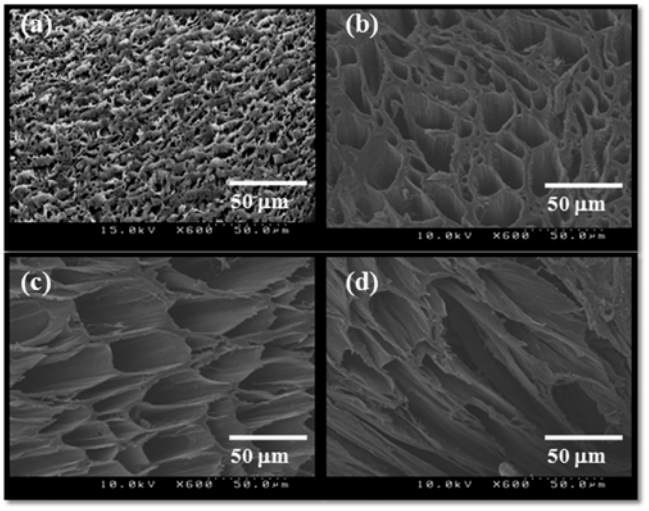

Figure 5. SEM photographs of UV irradiated PVA/Ag-zeolite hydrogels; Ag-zeolite content of (a) 0, (b) 1 wt%, (c) 3 wt%, and (c) 5 wt%.

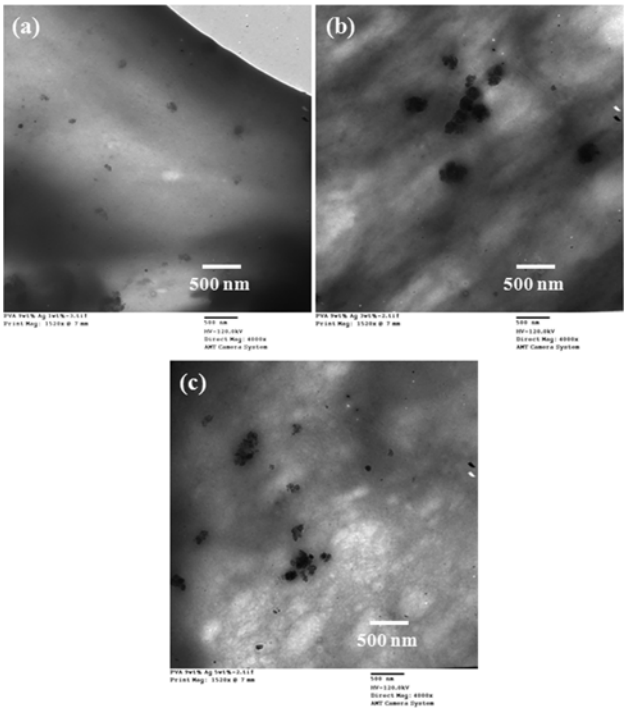

Figure 6. TEM photographs of UV irradiated PVA/Ag-zeolite hydrogels; Ag-zeolite content of (a) 1 wt%, (b) 3 wt%, and (c) 5 wt%.

changes in gel microstructure with polymer concentration. The micropores increased with increasing PVA concentration; thus, the pore size became smaller at higher polymer concentrations. The microporous structure was well developed on the surface of the PVA hydrogel with increasing UV-irradiation time. There are interconnections between micropores leading to sponge-like hydrogel structures, which is a general characteristic of the hydrogel. Hydrogels form hydrophilic three-dimensional network structures held together, where pores within the network allow water molecules to be trapped and immobilized; therefore, water fills the available free volume of the network. Based on the results of the present study, the concentration of PVA and irradiation time were fixed to 9 wt% and 10 min, respectively.

The gel fractions and swell ratios of PVA/Ag-zeolite composite hydrogels for different Ag-zeolite contents are shown in Figure 4. The gel fraction of PVA/Ag-zeolite composite hydrogels was lower than that of homo PVA hydrogel because the presence of Ag-zeolite particles between PVA polymer chains reduced the possibility of crosslinking. The gel fraction increased slightly with increasing Ag-zeolite content, which may have been due to aggregation of the Ag-zeolite particles at higher content.

Figure 4 also shows the swelling ratio of PVA/Ag-zeolite composite hydrogels. The swelling ratio of PVA/Ag-zeolite composite hydrogels was higher than that of homo PVA hydrogel. The swelling ratio increased with Ag-zeolite content to 1 wt%, above which it decreased slightly. The swelling capacity of PVA/Ag-zeolite composite hydrogel is related to the gel fraction and pore size.

Figure 5 presents the hydrogel morphology showing the interconnected microporous structure of PVA/Ag-zeolite hydrogels. The microporous structure of the PVA/Ag-zeolite hydrogels showed increase in pore size with increasing concentrations of Ag-zeolite. The pore size of homo PVA hydrogel is smaller than that of PVA/Ag-zeolite hydrogel; therefore, the swelling ratio of PVA/Ag-zeolite is higher than that of homo PVA hydrogels. In the case of PVA/Ag-zeolite

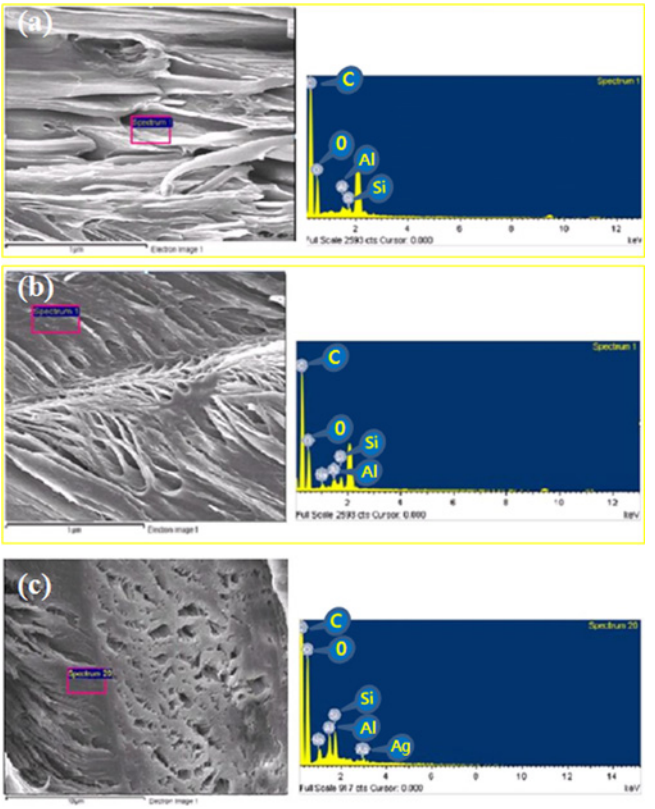

Figure 7. SEM photograph and EDS spectrum of PVA/Ag-zeolite hydrogels; Ag-zeolite content of (a) 1 wt%, (b) 3 wt%, and (c) 5 wt%.

composite, the pore size increased with increasing Ag-zeolite content (Figure 5), however, the maximum swelling ratio was observed at a Ag-zeolite content of 1 wt%, above which it decreased with increasing Ag-zeolite content. This may be attributed to the fact that, even though the pore size increases, the uniformity of pore size decreases at Ag-zeolite contents of 3 and 5 wt%, leading to decreased swelling. At the Ag-zeolite concentration of 5 wt%, micropores were squashed.

The presence of Ag-zeolite particles was revealed in the TEM images shown in Figure 6. Relatively uniform distribution in the hydrogel was observed at a Ag-zeolite content of 1 wt%. Ag-zeolite particles aggregated at higher Ag-zeolite content.

Figure 7 shows the EDS spectrum of a PVA/Ag-zeolite composite hydrogel. Carbon (C), silicone (Si) and aluminum (Al) are main components of the PVA/Ag-zeolite composite hydrogels. Ag ions were not detected at 1 and 3 wt% Ag-zeolite. This result might be attributed to the relatively small quantity of Ag ion particles in the zeolites (zeolite: 300,000 ppm, Ag: 10,000 ppm).

As shown in Figure 8, the DSC thermograms of the PVA/Ag-zeolite hydrogels had generally similar appearances.

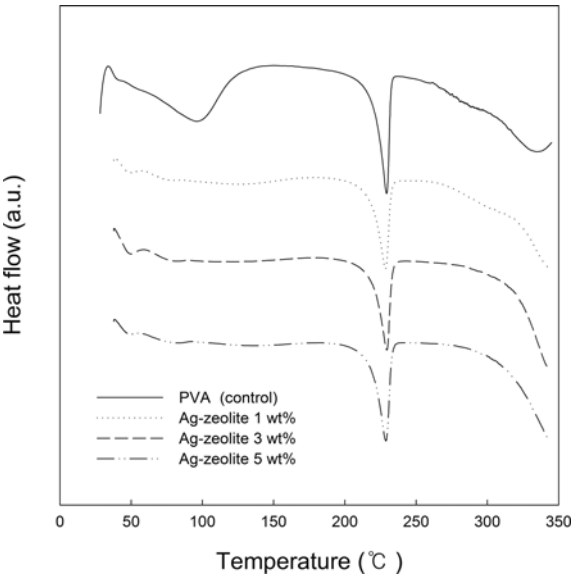

Figure 8. DSC thermograms of PVA/Ag-zeolite hydrogels.

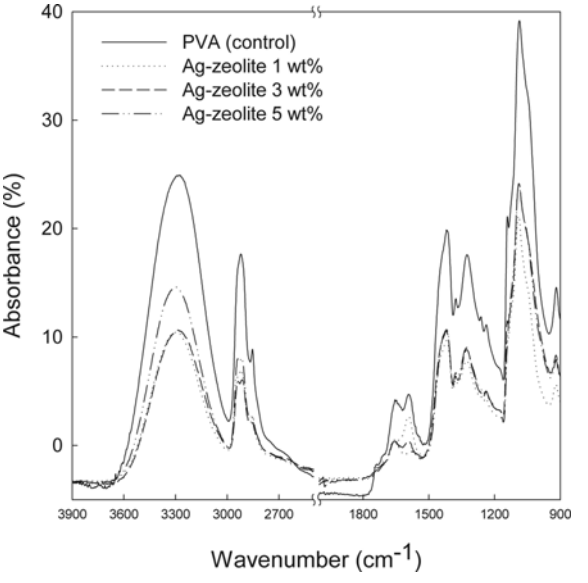

Figure 9. FT-IR spectrum of PVA/Ag-zeolite hydrogels.

Moreover, few changes in the melting temperature and heat of fusion were observed in the DSC thermograms, indicating no significant change in crystallinity in response to the addition of Ag/zeolite particles.

FT-IR spectra of PVA/Ag-zeolite composite hydrogels are shown in Figure 9. The characteristic peaks of PVA [27] revealed a band at 2800-3000 cm^{-1} for stretching vibrations of CH and CH_2 groups, a band at 1300-1500 cm^{-1} for CH/CH_2 deformation vibrations, a broad hydroxyl band at 3000-3600 cm^{-1}, and C-O stretching at 1000-1200 cm^{-1}. The absorption intensities of -OH stretching and -CH stretching bands of PVA/Ag-zeolite composite hydrogels were smaller

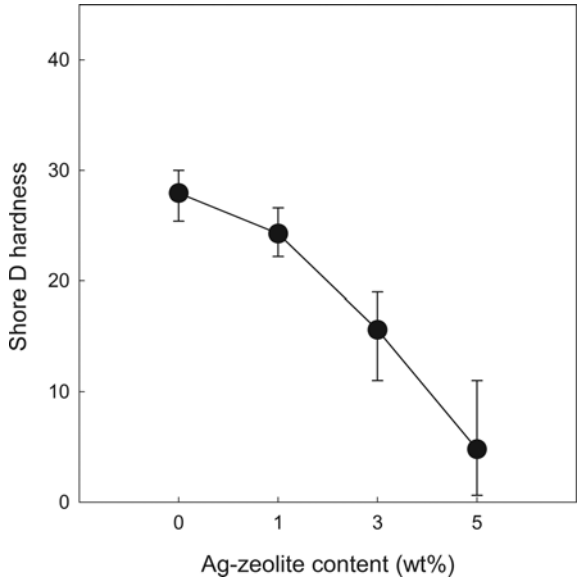

Figure 10. Shore D hardness of PVA/Ag-zeolite hydrogels.

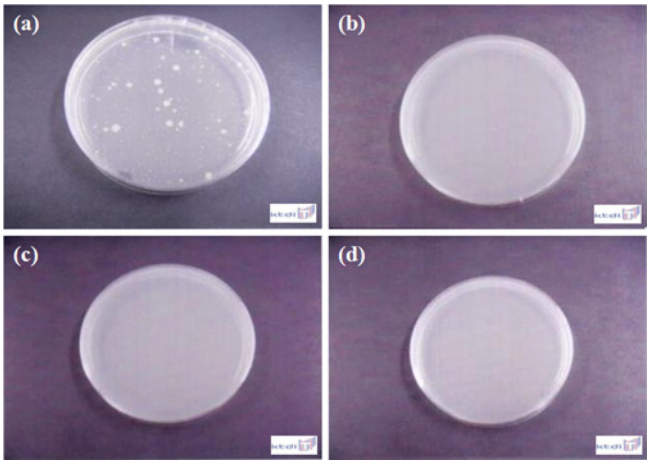

Figure 11. Photographs of antimicrobial activity of PVA/Ag-zeolite hydrogels against *Staphylococcus aureus*; Ag-zeolite content of (a) 0 wt%, (b) 1 wt%, (c) 3 wt%, and (d) 5 wt%.

than those of homo PVA. The addition of Ag-zeolite increased photo-oxidation rate by UV irradiation. Gaume *et al.* [27] reported that the FT-IR spectrum absorption intensity of -OH and -CH bands groups decreased with increasing UV irradiation time in comparison with no irradiation sample and the photo-oxidation rate of PVA was influenced by adding sodium monntmorillonite (MMt-Na^+) nano clay contents [28]. It can be inferred from decrease in the intensity of -OH and -CH absorption bands that addition of Ag-zeolite nanoparticles seems to affect the photo-oxidation rate of PVA/Ag-zeolite hydrogel and hence the morphology of hydrogels change as show in Figure 5.

Figure 10 shows the Shore D hardness, indicating resistance

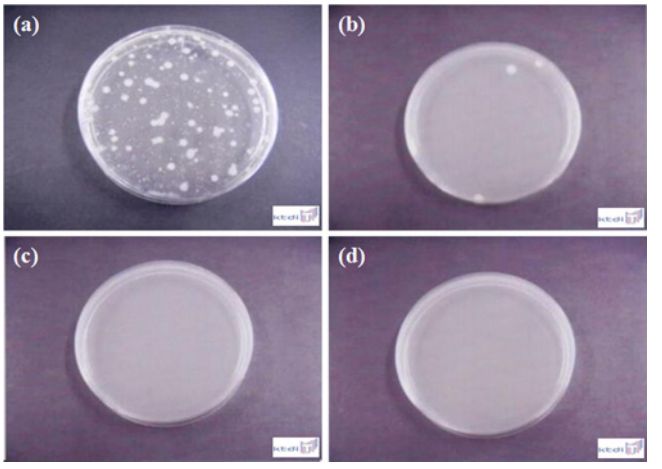

Figure 12. Photographs of antimicrobial activity of PVA/Ag-zeolite hydrogels against *Klebsiella pneumoniae*; Ag-zeolite content of (a) 0 wt%, (b) 1 wt%, (c) 3 wt%, and (d) 5 wt%.

Table 1. Reduction of bacteria of PVA/Ag-zeolite hydrogel against *Staphylococcus aureus* and *Klebsiella pneumoniae*

Ag-zeolite content (wt%)	Reduction of bacteria (%)	
	Staphylococcus aureus	*Klebiella pneumoniae*
0	0	8.6
1	99.9	99.8
3	99.9	99.9
5	99.9	99.9

of a material to the penetration of a needle under applied load. The Shore D hardness of PVA/Ag-zeolite composite hydrogels decreased with increasing Ag-zeolite content, leading to softer hydrogels at higher Ag-zeolite concentrations. This is because the PVA/Ag-zeolite composite hydrogels with larger Ag-zeolite contents have larger micropores (Figure 5). The Shore D hardness values of hydrogels containing 5 wt% Ag/zeolite were similar to those of very soft elastomers.

The antimicrobial activity of PVA/Ag-zeolite hydrogel against *Staphylococcus aureus* (Figure 11) and *Klebsiella pneumoniae* (Figure 12) was measured using the viable cell counting method. The PVA/Ag-zeolite hydrogel inhibited the growth of *Staphylococcus aureus* and *Klebsiella pneumoniae* (Table 1). The antimicrobial activity of the PVA/Ag-zeolite hydrogel against *Staphylococcus aureus* was 99.9 % at all Ag-zeolite contents, while it was 99.8 % for *Klebsiella pneumoniae* at a Ag-zeolite concentration of 1 wt% and over 99.9 % at 3 wt% and 5 wt%. These results show that the PVA/Ag-zeolite nanocomposite hydrogel had effective antimicrobial activity with small amounts of Ag-zeolite. The reduction of bacteria over 99.9 % is considered that it has the most effective antimicrobial activity [29]. The antibacterial reduction over 80 % is considered to be having antimicrobial activity [29]. Especially, in commercial production, the value of

99.9 % is important to assure antibacterial efficacy. More than 3 wt% of Ag-zeolite is needed to achieve sufficient antimicrobial activity.

Conclusion

PVA/Ag-zeolite hydrogels were prepared by UV irradiation of 365 nm at a PVA concentration of 9 wt% and UV irradiation distance of 15 cm for different Ag-zeolite contents. The pore size of PVA/Ag-zeolite hydrogels increased with increasing Ag-zeolite content. The PVA/Ag-zeolite hydrogels showed strong antibacterial activities against *Staphylococcus aureus* and *Klebsiella pneumoniae*, with antibacterial efficacy of over 99.9 % at a Ag-zeolite concentration of 3 wt%.

Acknowledgement

This research was supported by the Yeungnam University research grants in 2010.

References

1. T. Kanaya, M. Ohkura, K. Kaji, M. Furusaka, and M. Misawa, *Macromolecules*, **27**, 5609 (1994).
2. H. Takeshita, T. Kanaya, K. Nushida, and K. Kaji, *Macromolecules*, **32**, 7815 (1999).
3. T. Kanaya, H. Ohkura, K. Takeshita, K. Kaji, M. Furusaka, H. Yamaoka, and G. D. Wignall, *Macromolecules*, **28**, 3168 (1995).
4. J. M. Rosiak, P. Ulanski, L. A. Pajewski, F. Yoshii, and K. Makuuchi, *Radiat. Phys. Chem.*, **46**, 161 (1995).
5. D. K. Singh and A. R. Ray, *J. Appl. Polym. Sci.*, **66**, 869 (1997).
6. S. H. Hyun, W. I. Cha, Y. Ikada, M. Kita, Y. Ogura, and Y. Honda, *Biomater. Sci. Polym.*, **5**, 397 (1994).
7. J. H. Juang, W. S. Bonner, Y. J. Ogawa, P. Vacanti, and G. Weir, *Transplantation*, **61**, 1557 (1961).
8. N. A. Peppas and S. R. Stauffer, *J. Control Release*, **16**, 305 (1991).
9. N. A. Peppas and J. E. Scott, *J. Control Release*, **18**, 95 (1992).
10. T. Kanaya, H. Takeshita, Y. Nishikoji, M. Ohkura, K. Nishida, and K. Kaji, *Supramol. Sci.*, **5**, 215 (1998).
11. H. Takeshita, T. Kanaya, K. Nishida, and K. Kaji, *Macromolecules*, **34**, 7894 (2001).
12. B. Wang, M. Kodama, S. Mukataka, and E. Kokufuta, *Polymer Gels and Networks*, **6**, 71 (1998).
13. A. Carpi, "Hydorgels: Methods of Preparation, Characterisation and Applications in Progress in Molecular and Environmental Bioengineering - From Analysis and Modeling to Technology Applications", pp.132-139, InTech, New York, 2011.
14. S. Ichiro and I. Yoshito, *Bull. Inst. Chem. Res.*, **39**, 99 (1961).
15. J. Polavka, M. Uher, L. Lapcik, M. Ceppan, J. Valasek, and B. Havlinova, *Chem. Zvesti*, **34**, 780 (1980).
16. F. Yoshi, K. Makuuchi, D. Darmawan, T. Iriawan, M. T. Razzak, and J. M. Roasiak, *Radiat. Phys. Chem.*, **46**, 169 (1995).
17. M. Wu, B. Bao, F. Yoshi, and K. Makuuchi, *J. Radioan. Nuclear Chem..*, **250**, 391 (2001).
18. A. H. Clark and S. B. Ross-Murphy, "Biopolymers; Advances in Polymer Science", Vol. 83, Springer, New York, 1987.
19. H. Zheng, Y. M. Du, J. H. Yu, R. H. Huang, and L. N. Zhang, *J. Appl. Polym. Sci.*, **80**, 2558 (2001).
20. W. J. Li, C. T. Laurencin, E. J. Caterson, R. S. Tuan, and F. K. Ko, *J. Biomed. Mater. Res.*, **60**, 613 (2002).
21. Z. Hagiwara and S. Andou, *Aeolite*, **4**, 1 (1987).
22. E. R. Kenawy, G. L. Bowlin, K. Mansfield, J. Layman, D. G. Simpson, E. Sanders, and G. E. Wnek, *J. Controlled Release*, **81**, 57 (2002).
23. Z. M. Huang, Y. Z. Zhang, M. Kotaki, and S. Ramakrishna, *Comp. Sci. Technol.*, **63**, 2223 (2003).
24. S. A. Theron, E. Zussma, and A. L. Yari, *Polymer*, **45**, 2017 (2004).
25. H. G. Kim and J. H. Kim, *Fiber. Polym.*, **12**, 602 (2011).
26. J. Park, S. Lee. H. Kim, D. Won, D. Kim, K. Lee, H. Woo, and E. Kim, *J. Adhesion and Interface*, **12**, 81 (2011).
27. J. Gaume, P. Chung, A. Rivaton, S. Therias, and J. Gardette, *RSC Advances*, **1**, 1471 (2011).
28. J. Gaume, A. Rivation, S. Therias, and J. Gardette, *Polym. Degrad. Stab.*, **97**, 488 (2012).
29. H. C. Cha and Y. H. Kim, *J. Korean Fiber Soc.*, **45**, 214 (2008).